Sulfite reductase hemoprotein

M Elizabeth Stroupe and Elizabeth D Getzoff

in

Handbook of Metalloproteins

Edited by

Albrecht Messerschmidt, Robert Huber, Thomas Poulos and Karl Wieghardt

Sulfite reductase hemoprotein

M Elizabeth Stroupe and Elizabeth D Getzoff

The Scripps Research Institute, La Jolla, CA, USA

FUNCTIONAL CLASS

Enzyme; NADPH: oxidoreductase; EC 1.8.1.2; multimeric complex with iron-containing siroheme, [4Fe–4S] cluster; flavin adenine dinucleotide (FAD), and flavin mononucleotide (FMN); known as sulfite reductase (SiR).

Both dissimilatory and assimilatory sulfite reductases (dSiR/aSiR) use siroheme, a heme of the isobacteriochlorin class, coupled through an endogenous cysteine ligand to a [4Fe–4S] cluster to transform sulfite and nitrite to sulfide and ammonia, respectively.[1] Reducing equivalents come from a dissociable molecule of NADPH and bound flavins.[1]

OCCURRENCE

Sulfate reducing eubacteria and some archaebacteria use dSiRs as the terminal electron acceptor in anaerobic respiration.[2] Archaebacteria, bacteria, fungi, and plants all contain aSiRs. Animals lack an aSiR and therefore depend on plants to supply reduced sulfur for the biosynthesis of sulfur-containing amino acids and cofactors.[3]

BIOLOGICAL FUNCTION

The two classes of sulfite reductases perform distinct biological functions. DSiRs are $\alpha_2\beta_2$ heterotetramers that contain a total of two sirohemes and two iron–sulfur clusters,[3] although there are some discrepancies in the literature concerning the ratio of cofactor to subunits. Sulfate-reducing eubacteria and some archaebacteria use dSiRs to catalyze the final reductive step of anaerobic respiration, allowing these organisms to use sulfite as the terminal electron acceptor by transforming SO_3^{-2} to either sulfide (S^{-2}), trithionite ($S_3O_6^{-2}$), or thiosulfate ($S_2O_3^{-2}$).[2] DSiRs are distinguished from assimilatory SiRs (aSiRs) by

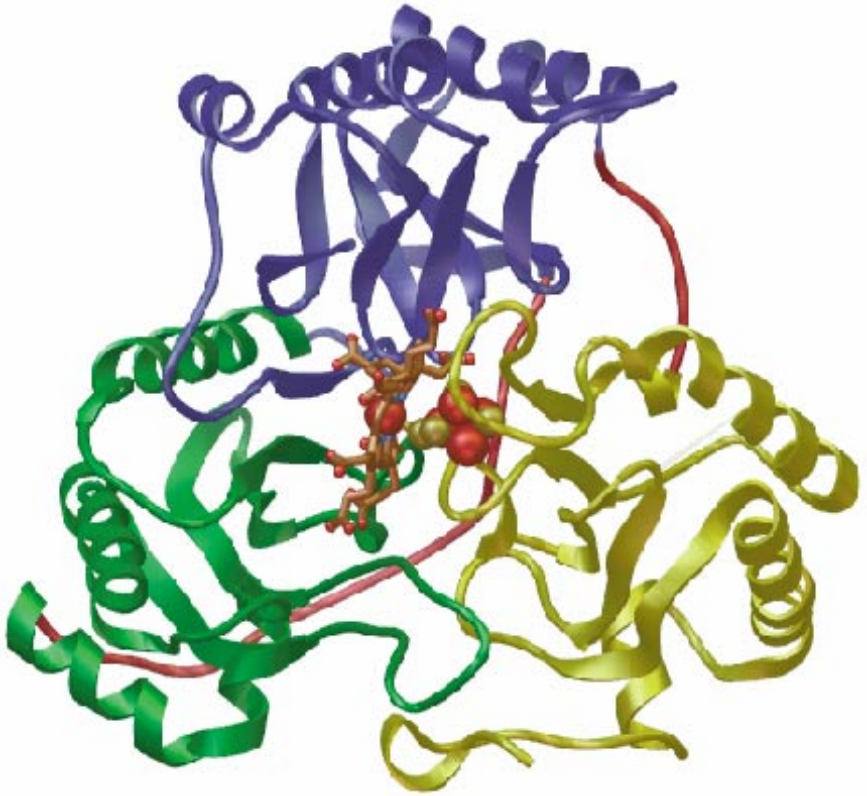

3D Structure Ribbon diagram of the hemoprotein from the assimilatory sulfite reductase (PDB code: 1AOP). The three domains are colored yellow, blue, and green and the linker is red. The siroheme is brown, irons are large red spheres, sulfur are yellow spheres, oxygens are red balls, and nitrogens are blue balls. Figure made using the Advanced Visualization Systems (AVS) package.[40]

function, subunit composition, and the product of the reduction. ASiRs are found in bacteria, archaebacteria, fungi, and plants and prepare sulfur for incorporation into sulfur-containing amino acids and cofactors.[3] Sulfur reduction by bacteria and plants is essential for transforming the inorganic element into a biocompatible form and for balancing the redox state of sulfur in the environment.[4,5] The NADPH-dependant $\alpha_8\beta_4$ complex performs the concomitant six-electron reduction to sulfide without releasing any partially reduced intermediates.[6] Sequence homology among the aSiR hemoprotein, both dSiR subunits, and ferredoxin-dependant nitrite reductases (NiRs) draw attention to five regions that define a conserved functional unit called the SNiRR (Sulfite or Nitrite Reductase Repeat) that is structurally important for the six-electron reduction catalyzed by the coupled siroheme/[4Fe–4S] cluster catalytic unit.[7] The crystallographic structure of the hemoprotein from *Escherichia coli* aSiR was solved to 1.6 Å resolution by Crane *et al.*[7] (3D Structure); the remainder of the article will focus on the hemoprotein from this assimilatory enzyme.

AMINO ACID SEQUENCE INFORMATION

- *Escherichia coli*, aSiR, flavoprotein (600 amino acid residues (AA)) and hemoprotein (572 AA), accession number (#): AAA23650 and AAA23651.[8,9]
- *Salmonella typhimurium*; aSiR, flavoprotein (599 AA) and hemoprotein (573 AA), #: AAA27046 and AAA27047.[8,9]
- *Thiocapsa roseopersicina*; aSiR, flavoprotein (522 AA) and hemoprotein (559 AA), #: CAA80687 and CAA80688.[10]
- *Arabidopsis thaliana* (thale cress); aSiR, 639 AA, #: CAA71239.[11]
- *Synechococcus PCC6301*; aSiR, ferredoxin-dependant, 625 AA, #: CAA77809.[12]
- *Synechococcus PCC7942*; aSiR, ferredoxin-dependant, 625 AA, #: P30008.[12]
- *Synechocystis PCC6803*; aSiR, ferredoxin-dependant, 635 AA, #: P72854.[13]
- *Saccharomyces cerevisiae* (budding yeast); aSiR hypothetical hemoprotein (481 AA), #: P47169 (M Rose, P Koetter and KD Entian, direct submission).
- *Desulfovibrio vulgaris (Hildenborough)*; dSiR, hemoprotein (219 AA), #: Q05805, from genomic DNA sequence.[14]

PROTEIN PRODUCTION, PURIFICATION, AND MOLECULAR CHARACTERIZATION

In the bacteria *E. coli* and *Salmonella typhimurium*, the *cys*I and *cys*J genes code for the hemoprotein and flavoprotein components of the holoenzyme aSiR. The genes are found as a single transcriptional unit (along with *cys*H, which codes for 3′-phosphoadenosine 5′-phosphosulfate sulfotransferase) in the cysteine regulon.Transcription of the three genes is under control of both the CysB protein and the co-inducers *O*-acetyl-L-serine or *N*-acetyl-L-serine and is activated in response to limiting sulfur.[9] *E. coli* aSiR can be recombinantly overexpressed from a pBR522-derived plasmid that contains the *cys*I, *cys*J, and *cys*G genes under the control of the endogenous promoter.[15] *Cys*G codes for siroheme synthase, a methyl transferase/iron cheletase that is necessary to make sufficient siroheme for forming fully metallated SiR.[15,16] *E. coli* aSiR is overexpressed in *S. typhimurium* that is *cys*I$^-$/*cys*J$^-$ and purified by protamine sulfate treatment followed by ammonium sulfate/calcium phosphate gel fractionation and ion exchange chromatography. SiRHP is isolated by dissociating the flavoprotein from the hemoprotein in 4 M urea and separating the two proteins over an anion exchange column.[9]

The macromolecular assembly of the aSiR holoenzyme, like other redox active proteins, funnels electrons from the cellular environment to the active site and substrate; each protein in the holoenzyme has a unique function. Eight copies of SiRFP and four copies of SiRHP form the 784 kDa holoenzyme.[1,17] SiRFP is a 66 kDa P450-like reductase and SiRHP is a 64 kDa protein that houses the active site. Both of the proteins bind a variety of cofactors.

METAL CONTENT AND COFACTORS

In the aSiR holoenzyme, each copy of SiRFP binds one molecule of FAD, one molecule of FMN, and one dissociable molecule of NADPH. In SiRHP, the active site is located on the distal side of a siroheme, which is coupled through its proximal cysteine ligand to a [4Fe–4S] cluster (Figure 1).[7,18] Siroheme is an iron-containing macrocycle of the isobacteriochlorin class that is derived from uroporphyrinogen III.[19]

The total iron content of the holoenzyme was determined using the wet ashing procedure of van de Bogart and Beinert.[1,20] The inorganic sulfide content was determined by treating the protein with an alkaline zinc reagent followed by spectroscopic quantification.[1] From these measurements, Siegel *et al.* deduced that there were four heme-associated irons, 16 non-heme irons, and 16 inorganic sulfides in the holoenzyme.[1] EPR and UV/vis spectroscopic measurements on the protein suggested that the heme-like cofactor was not of the porphyrin class and that the multiple metal sites were uniquely arranged in the protein. Murphy *et al.* identified the siroheme in subsequent biochemical studies;[21] however, the covalent juxtaposition of the cofactors was not fully characterized until the structure of the hemoprotein was solved.[7,18]

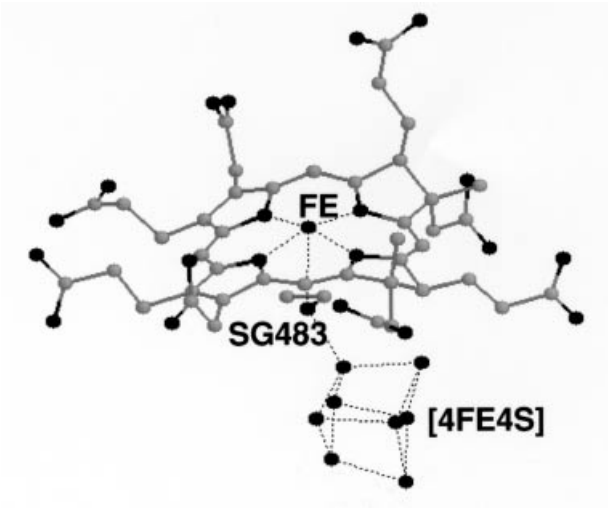

Figure 1 Ball and stick representation of the siroheme and [4Fe–4S] cluster cofactors. The figure was made using RASMOL.[41]

ACTIVITY ASSAY

Two assays are used to measure the SiR activity. The isolated holoenzyme catalyzes the reduction of sulfite, nitrite, or hydroxylamine by oxidizing NADPH, whose decrease in absorbance at 600 nm is monitored using UV/vis spectroscopy.[9] When separated from the holoenzyme, hemoprotein supplied with reducing equivalents from H_2/Pt asbestos-treated methyl viologen (MV^+) can reduce the substrate. The reaction is followed spectrophotometrically by monitoring the decrease of MV^+ at 450 nm.[22]

SPECTROSCOPY

Spectroscopy of SiRHP established an electronic couple between the siroheme and the [4Fe–4S] cluster that extends to the distally bound anion. Four distinct electronic states have been identified: oxidized, one- and two-electron reduced, and superoxidized. Characterization of these states using optical, EPR, Mössbauer, and resonance Raman (RR) spectroscopy are summarized in Table 1 and described in detail below.

Oxidized state

As isolated, the resting-state enzyme is oxidized and the associated optical and EPR spectra are consistent with a high-spin ferriheme and a diamagnetic $[4Fe–4S]^{2+}$ cluster. Optically, bands at 386 ($\varepsilon = 65.6\,mM^{-1}\,cm^{-1}$), 591 ($\varepsilon = 18.1\,mM^{-1}\,cm^{-1}$), and 714 ($\varepsilon = 5.6\,mM^{-1}\,cm^{-1}$) nm are attributed to the siroheme's Soret-, α-, and charge transfer (CT)-bands, respectively; EPR signals at $g = 6.63,\ 5.24,$ and 1.98 are indicative of an $S = 5/2$ species present at 5 K.[6] Mössbauer spectroscopy provides a slightly different view of the resting state of the enzyme that reveals the temperature-dependent behavior. At high temperatures, the spectrum is composed of a single quadrupole doublet ($\Delta E_Q = 1.00 \pm 0.10\,mm\,s^{-1}$) with an isomer shift (δ) of $0.37 \pm 0.05\,mm\,s^{-1}$ that is typical for both the high-spin ferrihemes and diamagnetic $[4Fe–4S]^{2+}$ clusters.[23] At low temperatures, a spectrum associated with the two distinct magnetic spin systems is measured. Specifically, the $S = 5/2$ ferriheme gives rise to a signal that ranges from -5 to 5 mm s^{-1}, while the second signal, which extends from -2 to 2 mm s^{-1}, is typical for a half-integral spin [4Fe–4S] cluster.[23] Christner *et al.* propose that the second paramagnetic spin system arises from a single unpaired spin (seen in the EPR spectrum as an $S = 5/2$ siroheme) that is shared between the siroheme and the [4Fe–4S] cluster.

RR spectroscopy on the hemoprotein's resting state predicted some of the siroheme's structural characteristics and recorded resonances for the [4Fe–4S] cluster. The spectrum derived from the excitation of siroheme at 406.7 or 568.2 nm, on the edge of the siroheme Soret- and α-bands, respectively, is more complex than that for an enzyme containing a protoporphyrin IX-derived heme because an isobacteriochlorin macrocycle has lower symmetry than a porphyrin macrocycle.[24] Han *et al.* suggest that the differences in vibrational modes between the enzyme-bound and free siroheme are because of nonplanarity, occupancy of its distal binding site, and coupling to the iron–sulfur cluster.[24] Resonances of the atoms on the [4Fe–4S] cluster were measured using ^{34}S-labeled enzyme excited at wavelengths typical for the excitation of [4Fe–4S] clusters (457.9 or 488.0 nm).[25] Although the cluster is linked through an endogenous cysteine ligand to the iron of the siroheme, no specific vibrational mode that can be attributed to $Fe_{[4Fe–4S]}$–S–$Fe_{siroheme}$(Fe_S) stretching is apparent from excitation at either the siroheme or cluster edge.

One-electron reduced state

SiRHP treated with one equivalent of MV^+ has distinct spectroscopic characteristics that are attributed to a one-electron reduced state in which both the siroheme and the [4Fe–4S] cluster are formally +2 while maintaining their electronic couple. Optically, the α-band broadens and the CT-band decreases in intensity.[26] In this state, both the hemoprotein and the [4Fe–4S] cluster are EPR silent, indicative of a ferrous siroheme and a diamagnetic cluster with a net charge of +2.[26] The Mössbauer spectrum of the one-electron reduced system was calculated by subtracting elements of the spectrum assigned only to the fully oxidized or fully reduced spectrum.[23] In agreement with the silent EPR spectrum, a zero or weak external magnetic

Table 1 SiRHP's formal redox states and their characteristic spectra

Formal redox state of cofactors	Optical spectrum λ (ε [mM^{-1} cm^{-1}])	EPR spectrum	Mössbauer spectrum: Temperature = 4.2 K, Field strength = 0 Tesla, 4 Tesla, 0.06 Tesla, 6.0 Tesla	Mössbauer spectrum: Temperature = 190 K, 140 K or 110 K or 195, Field Strength = 0 Tesla, 4 Tesla, 0.06 Tesla	Ref.
Siroheme = +3 Cluster = +2	384 nm (65.6) 588 nm (18.1) 710 nm (5.7)	g = 6.63, 5.24, and 1.98	Hyperfine signals: −5 to 5 mm s^{-1} −2 to 2 mm s^{-1}	Quadrupole doublet: $\Delta E_Q = 1.00 \pm 0.10$ mm s^{-1} $\delta = 0.37 \pm 0.05$ mm s^{-1}	39 26 23,27
Siroheme = +2 Cluster = +2	384 nm 588 nm 710 nm	Silent	Quadrupole doublet: $\Delta E_Q = 1.00 \pm 0.03$ mm s^{-1} $\delta = 0.45 \pm 0.02$ mm s^{-1} Quadrupole doublet: $\Delta E_Q = 1.92 \pm 0.06$ mm s^{-1} $\delta = 0.62 \pm 0.04$ mm s^{-1} Hyperfine signals	Quadrupole doublet: $\Delta E_Q = 1.72 \pm 0.04$ mm s^{-1} $\delta = 0.60 \pm 0.03$ mm s^{-1} Quadrupole doublet: $\Delta E_Q = 1.79 \pm 0.04$ mm s^{-1} $\delta = 0.61 \pm 0.03$ mm s^{-1}	26,27 30
Siroheme = +2 Cluster = +1	397 nm 608 nm	g = 2.53, 2.29, and 2.08 g = 5.23 and 2.80 g = 4.82 and 3.39 also g = 2.04, 1.93, and 1.91	Hyperfine signals	Quadrupole doublet convoluted with hyperfine signals	26
Siroheme = +4 Cluster = +2	386 nm (60.0) 590 nm (9.4) 714 nm (3.7)	Silent			31
Siroheme = +3 Cluster = +2 (CN^-)		g = 2.39, 2.33, and 1.67	Broad quadrupole doublet and hyperfine signals	Quadrupole doublet: $\Delta E_Q = 1.35 \pm 0.08$ mm s^{-1} $\delta = 0.19 \pm 0.05$ mm s^{-1}	28
Siroheme = +2 Cluster = +2 (CN^-)	404 nm 581 nm		Quadrupole doublet: $\Delta E_Q = 1.00 \pm 0.03$ mm s^{-1} $\delta = 0.45 \pm 0.02$ mm s^{-1} hyperfine signals		28
Siroheme = +2 Cluster = +1 (CO or CN)		g = 2.029, 1.925, and 1.910	(CO) Quadrupole doublet: $\Delta E_Q = 0.80 \pm 0.03$ mm s^{-1} $\delta = 0.23 \pm 0.02$ mm s^{-1} hyperfine signals (CN) Quadrupole doublet: $\Delta E_Q = 0.72 \pm 0.05$ mm s^{-1} $\delta = 0.39 \pm 0.03$ mm s^{-1} hyperfine signals	Quadrupole doublet: $\Delta E_Q = 0.70 \pm 0.03$ mm s^{-1} $\delta = 0.47 \pm 0.02$ mm s^{-1} Quadrupole doublet: $\Delta E_Q = 1.80 \pm 0.30$ mm s^{-1} $\delta = 0.59 \pm 0.02$ mm s^{-1}	28,30

field at low temperatures gives rise to a Mössbauer spectrum composed of two quadrupole doublets with splittings and isomer shifts that correspond to the diamagnetic $[4Fe–4S]^{2+}$ cluster (1.00 ± 0.03 and 0.45 ± 0.02 mm s^{-1}, respectively) and a ferroheme iron (1.92 ± 0.06 and 0.62 ± 0.04 mm s^{-1}).[23,27] The siroheme iron is paramagnetic and of integral spin, $S = 1$ or 2, supported by the evidence of hyperfine interaction between the cluster and siroheme iron observed when the spectrum is acquired in a strong external magnetic field.[27] Christner *et al.* remind us that the addition of one electron changes the spectra of five distinct iron atoms, further supporting the hypothesis that the metal sites are exchange coupled throughout the enzyme's redox cycle.[23,27]

Two-electron reduced state

The spectra of the two-electron reduced enzyme are consistent with a spin-coupled system in which the formal charge on the siroheme's iron is +2 ($S = 1$ or 2) and on the [4Fe–4S] cluster is +1 ($S = 1/2$). The Soret band shifts to

397 nm and a broad α-band is centered at 608 nm. The EPR spectrum is complex, with three sets of signals at g = 2.53, 2.29, and 2.08; g = 5.23 and 2.80; and g = 4.82 and 3.39 as well as a set of signals at g = 2.04, 1.93, and 1.91.[26] At higher temperatures, the Mössbauer spectrum shows a quadrupole doublet that resembles the one-electron reduced spectrum and is assigned to the ferro-heme, supporting the hypothesis that the second electron is added to the cluster because the high-temperature siro-heme spectrum remains essentially unchanged from the one- or two-electron reduced species. Regardless of the strength of the applied magnetic field, at low temperatures the Mössbauer spectrum exhibits a large number of hyperfine interactions that arise from coupling between the cluster and the siroheme irons, describing a system composed of two half-integral spins.[27] In conclusion, the second electron is formally placed on the cluster, however spin-coupling between the cofactors allows the half-integral, unpaired spin to delocalize across all five iron ions.

Inhibitor complexes

Binding of small molecules to the siroheme changes the spectroscopic properties and affects the spin state of the iron centers. When a strong-field ligand such as CO or CN^- binds to the two-electron reduced enzyme, back-bonding between the π-orbitals of the anion and the *d*-orbitals of the metal changes the siroheme iron from a high-spin to a low-spin configuration, as indicated by an EPR spectra showing only a pure g = 1.94 signal that is attributed to a paramagnetic $[4Fe–4S]^{1+}$ cluster and an optical spectra with bands at 404 and 581 nm but with no CT band.[6] The low-temperature, zero-field Mössbauer spectrum of the CO adduct with the doubly reduced enzyme shows two signals.[28] A strong quadrupole doublet is assigned to the low-spin, diamagnetic siro-heme iron based on its quadrupole splitting of 0.80 ± 0.03 mm s^{-1} and isomer shift of 0.23 ± 0.02 mm s^{-1}. The paramagnetic $[4Fe–4S]^{1+}$ cluster gives rise to a broad multiplet. At high temperatures and in the absence of an external magnetic field, two quadrupole doublets arise from two pairs of equivalent irons in the paramagnetic $[4Fe–4S]^{1+}$ cluster (ΔE_Q = 0.70 ± 0.03 mm s^{-1} and δ = 0.47 ± 0.02 mm s^{-1}, and ΔE_Q = 1.80 ± 0.30 mm s^{-1} and δ = 0.59 ± 0.02 mm s^{-1}).[28]

On the contrary carbon monoxide only binds to the reduced enzyme, cyanide binds regardless of the enzyme's oxidation state and each redox state has a slightly different spin distribution. As in the reduced complex, the EPR spectrum of the oxidized, CN-bound enzyme (signals at g = 2.39, 2.33, and 1.67) indicates that the siroheme contains a low-spin ferric iron.[28] The Mössbauer spectrum of this state shows a temperature dependent behavior, where the low-temperature spectrum shows a broad quadrupole doublet and undefined hyperfine interactions between the cluster and siroheme irons; and the high temperature spectrum shows a sharp doublet as a result of the diamagnetic irons in the cluster and siroheme (ΔE_Q = 1.35 ± 0.08 mm s^{-1} and δ = 0.19 ± 0.05 mm s^{-1}).[28] When the enzyme is one-electron reduced, the cyanide complex produces a Mössbauer spectrum with only a sharp quadrupole doublet, suggesting that all five irons are diamagnetic; like the EPR spectrum, the Mössbauer spectrum of the doubly reduced CN^- adduct looks like that of the CO complex.[28] Additionally, the redox couples of both cofactors change on ligand binding (the siroheme +3/+2 couple is about −155 mV and the cluster +2/+1 couple is about −490 mV in the cyanide complex; the cluster +2/+1 couple is about −420 mV in the carbon monoxide complex compared to the resting-state vales of −340 and −405 mV), suggesting that binding to the siroheme also affects the [4Fe–4S] cluster.[6,26]

RR spectra of the enzyme-bound CO^-, CN^-, and NO excited at wavelengths associated with siroheme absor-bances have lower X–Y stretching frequencies than those measured for the free anion.[29] The decrease in stretching energy could be caused by interactions between the anions and protein side chains in the active site. Mixed Fe–X–Y bending modes seen in the spectra suggests a multiplicity of anion binding conformations, possibly due to a mixture of redox states in the sample.[29]

Substrate complexes

SiRHP reduces sulfite and nitrite, both of which bind slowly to the resting-state enzyme and quickly to the reduced enzyme. When sulfite binds to the fully reduced enzyme, the complex absorbs optically at 396 and 592 nm and if the reduced complex is reoxidized with ferricyanide, the complex absorbs at 408 and 583 nm. Both the complexes are EPR silent, suggesting that in the two-electron reduced complex electron transfer to the substrate has occurred, leaving a diamagnetic [4Fe–4S] cluster.[30] Nitrite binds to the one- or two-electron reduced enzyme and nitric oxide binds to the oxidized or one-electron reduced enzyme, providing two ways of generating equivalent species (NO_2^- bound to two-electron reduced enzyme is the same as NO bound to one-electron reduced enzyme, and NO_2^- bound to one-electron reduced enzyme is the same as NO bound to the oxidized enzyme) to show that regardless of how the complex was generated the optical and EPR spectra are identical.[30] Specifically, the NO_2^--bound two-electron reduced enzyme absorbs opti-cally at 400 and 599 nm and has EPR signals at g = 2.12, 2.07, 2.01, and 1.996, suggesting that the cofactors still have some EPR-active properties.[30] When the one-electron reduced NO_2^- complex is treated with ferricyanide, the resulting oxidized complex absorbs optically at 399 and

581 nm with minor EPR signals at g = 2.01 and 2.0, g = 4.3, and g = 6.63 and 5.25.[30]

Superoxidized state

In addition to the one- and two-electron reduced states, the enzyme goes through a spectroscopically distinct state when the resting-state enzyme is further oxidized with porphyrexide (4-amino-2,5-dihydro-2-imino-5,5-dimethyl-1*H*-imidazol-1-yloxy).[31]

The relative energies of the highest occupied molecular orbital (HOMO) and the lowest unoccupied molecular orbitals (LUMO) from the siroheme iron, the isobacteriochlorin ring, and the iron–sulfur cluster (measured by optical, Fourier-transform infrared, ^{1}H NMR, and EPR spectroscopy and cyclic voltammetry on model complexes)[32] suggest that the oxidation occurs at the macrocycle and not at an iron; however there is little evidence that this superoxidized intermediate plays a role in the enzyme's mechanism. The intermediate is EPR silent and the three optical bands are slightly blue-shifted with a decrease in the intensity of their absorbance.[31]

CRYSTALLOGRAPHY AND STRUCTURE OF NATIVE SIRHP

Crystallography and single-crystal spectroscopy

Crystals of SiRHP grow from 15% PEG 8000, pH 7.7 (65 mM potassium phosphate), and 100 μM EDTA when the first 73 residues are cleaved by trypsin digest.[7] Phases were determined from an ethyl mercurithiosalicylate (ETMS) derivative supplemented with the low-resolution data from four other heavy metals. The above phases were combined with those determined from the two multi-wavelength anomalous diffraction experiments performed on the five native irons and the selenomethionine-substituted protein, allowing the 1.6 Å resolution structure to be refined to an R_{factor} of 19.1% and an R_{free} of 21.8%.[7,33,34] Crystals of reduced enzyme were produced either by soaking anaerobically with Cr(II)EDTA or by photoreduction in a solution containing 750 μM proflavin.[35,36] Substrates, intermediates, and inhibitors were soaked into either native or reduced crystals. The redox state of the metal was confirmed by comparing single crystal EPR spectra of capillary-mounted crystals in an EPR tube with spectra recorded from the same crystals after being exposed to air.

Description of the overall fold

SiRHP is a trilobed protein with pseudo two-fold symmetry; as shown in the 3D Structure, the green domain (domain 2; residues 146–346) relates to the yellow domain (domain 3; residues 422–570) through a two-fold axis down the middle of the blue domain (domain 1) that also relates subdomain 1 (residues 81–145) to subdomain 1′ (residues 347–421).[7] The molecule is about 60 Å wide and about 40 Å thick, with the cofactors bound at the junction of the three domains. Domain 1 resembles a parachute in which two central antiparallel β-sheet 'cords' link the α-helical 'canopy' to the 'harness-like' hairpin loops. Four α-helices sit at the solvent-accessible periphery while the loops supply the residues whose side chains form hydrogen bonds with acetyl and propionyl groups from the siroheme. Domains 2 and 3 are composed of a central five-stranded β-sheet that is surrounded by the three solvent-exposed α-helices. In the β-sheet, the fourth strand runs antiparallel to the first, second, third, and fifth strands. Side chains from

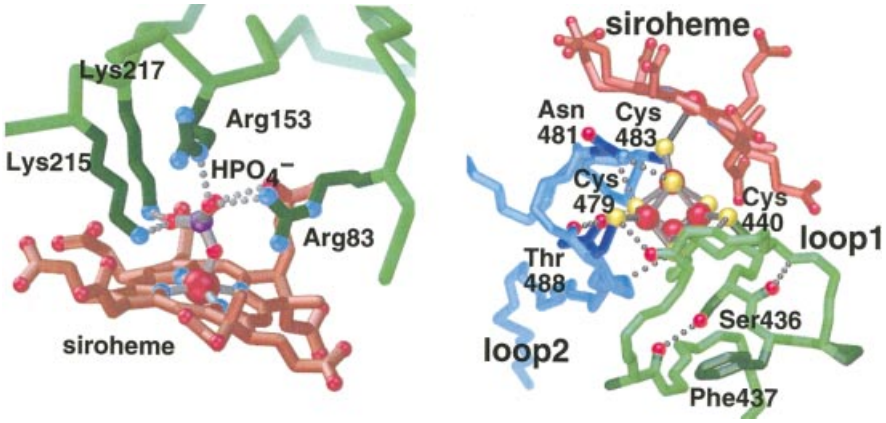

Figure 2 (a) The distal face of the siroheme in which the iron of the siroheme is formally +3 and the [4Fe–4S] cluster is formally +2. The three sidechains that form hydrogen bonds with the bound phosphate are green, the phosphorus of the anion is purple, oxygens are red balls, nitrogens are blue balls, and the iron is a large red sphere. Hydrogen bonds are depicted by gray balls. (b) The proximal face of the siroheme (brown) in which the iron of the siroheme (a large red sphere) is formally +3 and the [4Fe–4S] cluster is formally +2. Loop 1, the lariat, is green and loop 2 is blue. Sulfurs are yellow spheres, oxygens are red balls, nitrogens are blue balls, and hydrogen bonds are gray balls. Both figures are made in AVS.

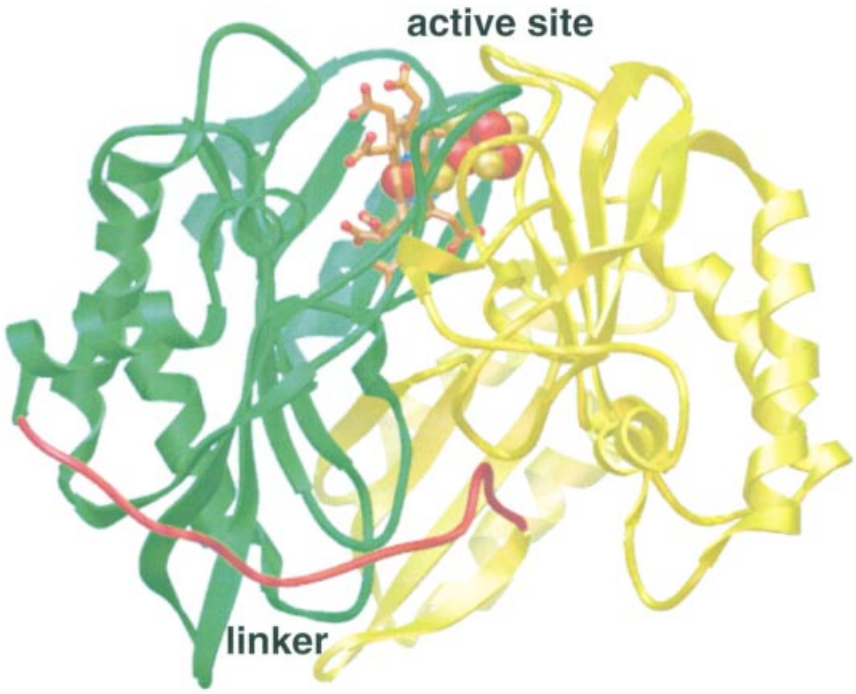

Figure 3 A ribbon diagram of the hemoprotein colored to show the two halves of the pseudosymmetric dimer, with the active site sitting in a channel towards the protein surface. The linker is a red tube, irons are large red spheres, sulfurs are yellow spheres, and the siroheme is brown. Figure made in AVS. This orientation is roughly 90 degrees from the 3D structure as viewed from the bottom.

Arg83, Arg153, Lys215, and Lys217, found in domain 2, line the active site and create a positively charged cage for the substrate on the distal side the siroheme (Figure 2(a)). Two loops from domain 3 surround the [4Fe–4S] cluster and donate the four cysteines (Cys434, Cys440, Cys479, and Cys483) that coordinate the irons of the cluster (Figure 2(b)). In the second loop, a tight $CysX_3Cys$ turn places Cys483 as the bridge between the cluster and the siroheme. Salt bridges between Glu448 (found in the first cluster loop) and both Arg336 from domain 1 and Arg113 from the strand that links domains 2 and 3 help form the domain interface. Additionally, a number of loops and turns that connect the β-strands and α-helices within each domain point towards the domain interface. Finally, the central position of the cofactors draws the domains together because each domain plays a role in coordinating the cofactors. A long linker holds together the two halves of the pseudosymmetric fold (Figure 3). Residues 340–345 play a unique role in the linker because they seem to mimic the siroheme's interactions with the protein scaffold, suggesting that the hemoprotein once housed two active sites related by the two-fold pseudosymmetry (Figure 4). In particular, when one half of the molecule is superimposed on the other half, Arg342 (shown, along with the other linker chain, in blue) aligns with the most axial propionate group (shown, along with the siroheme, in brown) while the backbone of Gly341 and Thr340 take the place of the

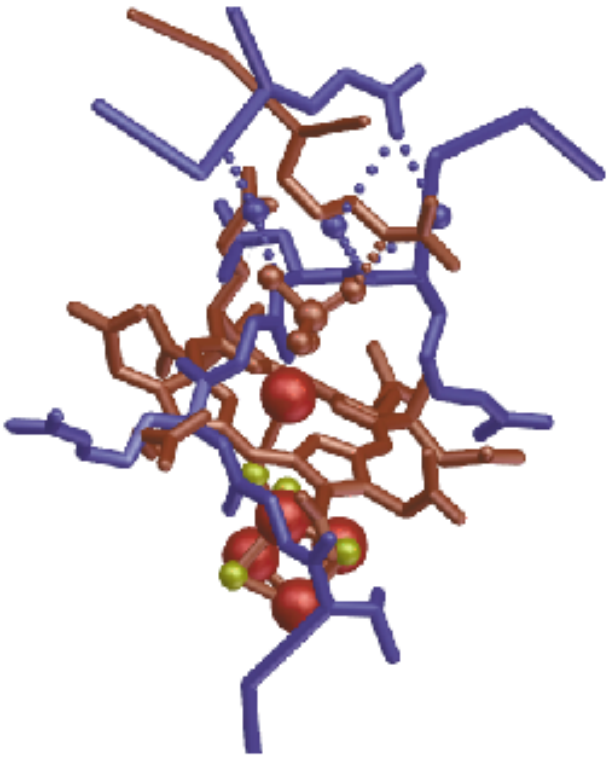

Figure 4 Overlay of the siroheme (brown) with sidechains from the linker (blue). Figure made in AVS.

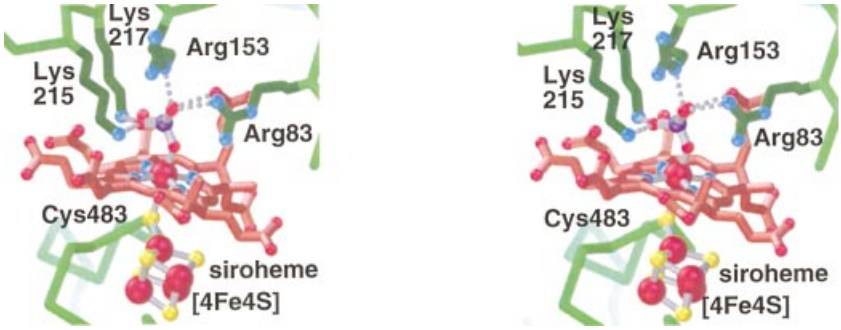

Figure 5 Stereo view of the active site of SiRHP showing both the distal and proximal sides of the siroheme. The siroheme is brown, irons are large red spheres, sulfurs are yellow spheres, phosphate is purple, nitrogens are blue balls, oxygens are red balls, and hydrogen bonds are gray balls. Figure made in AVS.

isobacteriochlorin ring. The side chain from Asp344 mimics another siroheme propionate group and its backbone fills the same space in the pseudosymmetric linker as does the bound phosphate in the active site.

Arrangement of the active site in the oxidized enzyme

In the structure of oxidized SiRHP, the siroheme sits at the pseudo-two-fold axis with a distally bound phosphate (Figure 5).[7] The phosphate binds to the siroheme's iron through an oxygen with a bond length of 1.88 Å. A single P–O bond is about 0.2 Å longer than the others and it is involved in a long hydrogen bond (about 2.7 Å) with a siroheme propionate, suggesting that the bound phosphate is singly protonated.[36] The average Fe–N distance in the resting form of the enzyme is about 2.11 Å and the separation between the Fe_S–Fe4 is about 4.48 Å.

The Fe_S is covalently bonded to Cys483 S_γ with a bond length of about 2.84 Å and the iron in the siroheme is domed out of the plane formed by the coordinating nitrogens by about 0.30 Å, characteristic of the high-spin heme irons.[7] As the RR spectroscopy predicted, the siroheme is significantly bowed, reducing the central macrocycle's symmetry to that of the S_4 point group.[24] On the proximal side of the siroheme, Cys483 bridges the siroheme iron to Fe4 from the cluster. Relative to the polypeptide backbone, Cys483 is in a strained position, however with respect to the siroheme its geometry can be reasoned to stagger the Cys483 S_γ–C_β bond with the siroheme's NC–Fe and NB–Fe bonds.[36]

Additionally, the thiolate lone pair from the bridging sulfur is positioned parallel to the siroheme-iron's d_{xy}-orbital, pointing roughly between the iron's downward-projecting d_{xz}- and d_{yz}-orbitals and providing a mechanism for orbital overlap between Cys483 S_γ's p-orbitals and the metal's d-orbitals. The bowed siroheme brings its CHB within van der Waals contacts of one of the sulfide atoms in the [4Fe–4S] cluster, suggesting there may be more than one path through which electrons can move from one cofactor to the other. At 1.6 Å resolution, a slight asymmetry in the cluster geometry places the Cys483-coordinated Fe4 about 0.05 Å closer to Fe1 than any other iron is to any other. Crane *et al.* suggest that the geometric distortion may be caused by exchange coupling between the cluster, allowing the siroheme to draw electrons out of the cluster and possibly alleviate the charge repulsion in the [4Fe–4S] cluster. Another cause for the distortion, they suggest, could be that the protein environment promotes the especially close packing of the cluster to the siroheme.[36]

Cluster tuning by loop 1

The loops that donate the cysteine thiolates to coordinate the [4Fe–4S] cluster also tune the cluster's chemical properties through interactions between the side- and main-chain atoms and the cluster's sulfurs.[36] In the structure of the hemoprotein, the first 'lariat-like' loop helps form the domain interface, described above, and protects the cluster from the solvent (Figure 2(b)). An unusual tight turn in this loop caps the cluster and places Phe437 in a strained conformation, seemingly projected

Table 2 Catalytic parameters for *E. coli* SiR

Substrate	K_M (mM^{-1})	k_{cat} (electron s^{-1} $heme^{-1}$)	k_{cat}/K_M (electron M s^{-1} $heme^{-1}$)	V_{max} (MV^+min^{-1} $heme^{-1}$)	Reference
SO_3^{2-}	1.2×10^{-2}	43.3	3.6×10^6	2.6×10^3	6
NO_2^-	1.5	98.3	6.5×10^4	5.9×10^3	6
NH_2OH	10.5	7.5×10^2	7.1×10^4	4.5×10^4	6

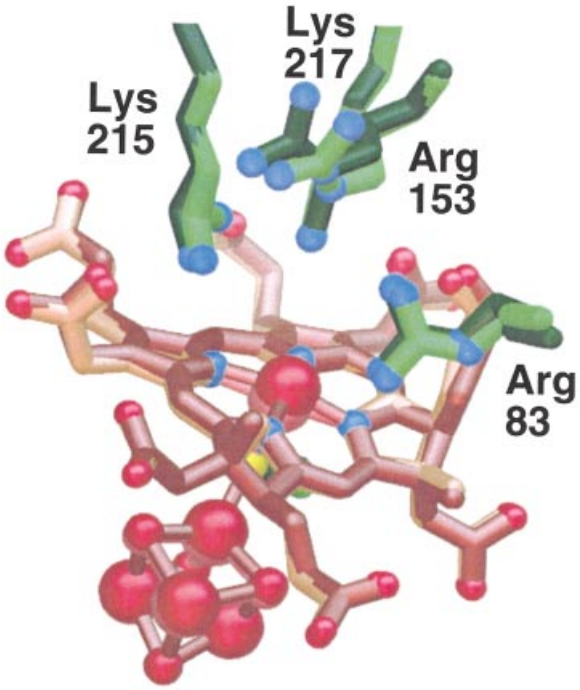

Figure 6 Overlay of the fully oxidized (siroheme is brown, irons and cluster are dark red, sidechains are dark green) and fully reduced metal cofactors (siroheme is creme, irons and cluster are pink sidechains are light green). The bound anion in the fully oxidized structure is excluded. Figure made in AVS.

into solution. Electrostatic calculations on the protein surface show a large, positively charged patch to which the first loop contributes.[7] Internally, hydrogen bonds form between the cluster's inorganic sulfurs and Ser436's main-chain nitrogen (from the first loop); side-chains from Asn481 and Thr488 (from the second loop); and main-chain nitrogens from Cys483, Gly482, and Cys479 (from the second loop). Therefore the loops' role is two fold: first, the flavoprotein may dock on the positively charged surface and interactions with the first loop could mediate electron transfer across the subunit interface; second, the iron–sulfur cluster solvation and hydrogen-bonding patterns affect the cluster's redox potential, thus the loops may help tune the redox potential of the cluster.

FUNCTIONAL ASPECTS

Kinetics and binding

Although sulfite, nitrite, and hydroxylamine have similar chemical structures, they bind with different affinities to the active site of SiRHP and their rates of catalysis by the enzyme are different (Table 2). SiRHP selects for sulfite over nitrite by binding it about 2 orders of magnitude better (K_M for sulfite is 1.2×10^{-2} mM^{-1} and for nitrite it is 1.5 mM^{-1}) and hydroxylamine binds the weakest, with a K_M of 10.5 mM^{-1}.[6] While the nitrogen-containing substrates bind with weaker affinity, the k_{cat} for their reduction is faster than for the sulfur-containing substrates, however, overall the enzyme is most efficient at reducing sulfite.

RELATIONSHIP BETWEEN STRUCTURE AND REDOX STATES: IMPLICATIONS FOR CATALYSIS

The structure of the resting form of SiRHP answered the long asked question regarding the covalent interactions between the two metallic cofactors. Structures of the fully and partially reduced hemoprotein and structures of the hemoprotein in complex with inhibitors, substrates, and intermediates unequivocally established that the siroheme and [4Fe–4S] cluster maintained their covalent interaction throughout the redox cycle while supporting a view in which the electronic couple of the cofactors extends to the bound anion.

Redox states

Stoichiometric reduction of the crystals was difficult as prolonged exposure to the reductant caused the crystals to decay, however EPR spectroscopy was used to monitor the extent to which the reduction occurred during short soaks to generate a series of structures that correlate with the previously characterized spectroscopic states.[35,36]

One-electron reduced state

Proflavin-treated crystals that are photoreduced for a short period of time have an EPR spectrum that corresponds to the one-electron reduced state characterized in solution.[36] Compared with the structure of the resting state of the enzyme, the Fe_S moved into the plane of the siroheme nitrogens, shortening the Fe_S–Cys483 S_γ bond length to 2.68 Å and decreasing the extent of the siroheme's dome to about 0.23 Å out of the nitrogen plane. The average N–Fe_S bond length is shorter than in the oxidized structure at about 2.04 Å. The Fe_S–Fe4 separation is about 4.35 Å in the partially reduced structure, about a half an Angstrom closer than in the fully oxidized state. The density on the distal side of the siroheme was well modeled by a phosphate molecule and a water molecule each at half occupancy, suggesting that release of the phosphate is linked to the redox state of the enzyme.

Two-electron reduced state

The structure of the fully reduced enzyme suggests a mechanism to explain the observation that anions bind

Table 3 Summary of the geometry of anion bonding in SiRHP and PDB codes

Structure	S–SFe (Å)	SFe–Fe4 (Å)	Dome SFe (Å)	Fe–X (Å)	Average N–SFe (Å)	PDB code (reference)
HP–PO_4	2.84	4.48	0.30	1.85	2.11	1AOP (7)
HP–PO_4 (proflavin/pr)	2.68	4.35	0.24	1.85	2.07	4AOP (36)
HP (empty)	2.37	4.13	0.01	N.A.	2.03	5AOP (36)
HP–CN	2.23	2.31	0.09	1.84	2.04	4GEP (35)
HP–CO	2.23	2.29	0.13	1.62	2.12	5GEP (35)
HP–SO_3	2.34	2.28	0.11	2.20	2.05	2GEP (35)
HP–S(X)	2.48	2.23	0.13	2.34	2.02	7GEP (35)
HP–NO_2	2.45	2.23	0.08	2.00	2.06	3GEO (35)
HP–NO	2.65	2.21	0.18	1.76	2.06	6GEP (35)
HP–NO_3	2.64	2.22	0.21	3.10	2.11	8GEP (35)

faster to the reduced enzyme than to the oxidized enzyme. In the presence of excess phosphate, structural changes in the fully reduced enzyme are not significantly different from those in the one-electron reduced enzyme; the Fe_S–Cys483 S_γ separation is 2.69 Å and the siroheme is domed by about 0.18 Å. The distance between Fe_S–Fe4 is the same as it is in the partially reduced structure, as is the average N–Fe_S distance. The phosphate molecule remains bound. When the experiment was repeated on protein crystallized in hepes buffer (pH = 7.7) instead of phosphate buffer, however, the distally bound phosphate is absent, the iron is in the plane of the siroheme nitrogens so that the siroheme is only domed by 0.01 Å, and a loop, which sits above the active site, is disordered. Other bond lengths are shorter in the fully reduced structure than in the partially reduced and fully oxidized structure: the Fe_S–Cys483 S_γ distance is only about 2.23 Å, the Fe_S–Fe4 separation is about 4.13 Å, and the average N–Fe_S distance is about 2.03 Å (Figure 6).

The changes in the active site on reduction support the two hypotheses about how the enzyme works. First, in the oxidized state of the enzyme, the phosphate competes with substrate for binding to the Fe_S but it is released when the enzyme is reduced. The phosphate seems to act as a steric block to keep the substrate from binding when the enzyme is not primed for catalysis by reduction. Second, tighter

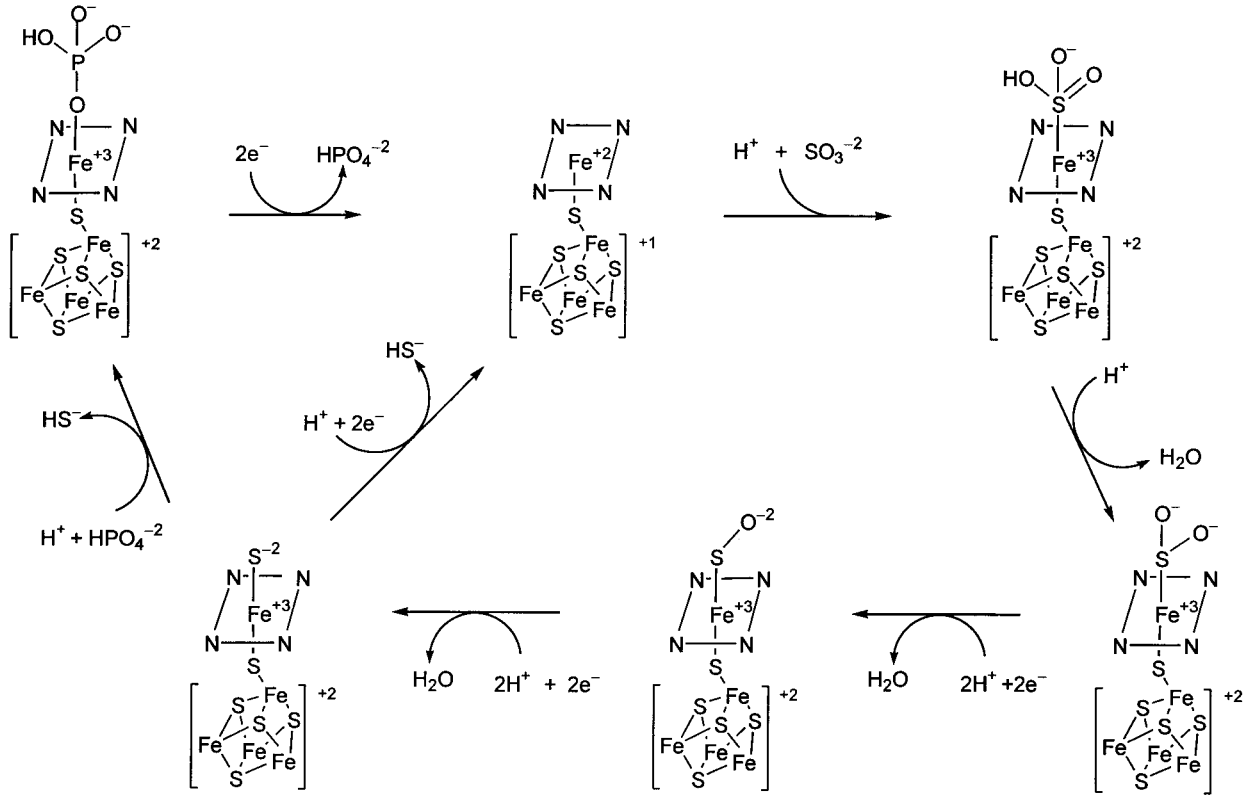

Figure 7 Schematic for the proposed mechanism of sulfite reduction by aSiRHP.

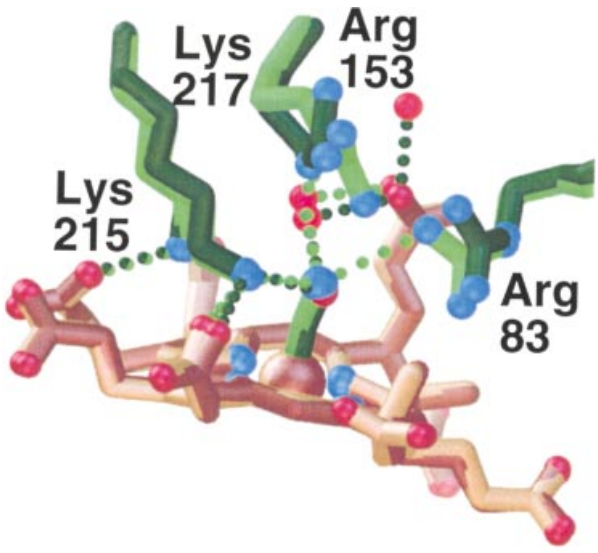

Figure 8 Overlay of the distal face of the siroheme with CO (siroheme is brown, sidechains and CO are dark green) and CN^- (siroheme is creme, sidechains and CN^- are light green) bound. Figure made in AVS.

association of the cofactors upon reduction and subsequent release of bound ligand suggests that anions binding to the siroheme's distal face compete with the bridging cysteine for the iron's bonding orbital and promotes the hypothesis that the cofactor couple extends to the bound anion.

Active site flexibility

One of the unique properties of the assimilatory SiR enzyme is its ability to reduce inorganic sulfite by six electrons without releasing intermediates, in spite of the relatively large changes in the substrate geometry. The structure of the oxidized enzyme suggests that the positively charged side chains lining the active site play a role in binding anions. The series of structures of the hemoprotein in complex with a variety of ligands elucidates how subtle differences in the exogenous ligands affect binding and catalysis. Table 3 summaries the details from the structures and their protein data bank codes.

From the above structures, Crane *et al.* proposed a possible mechanism for the six-electron reduction of sulfite by SiRHP.[35] According to their mechanism (Figure 7), the first two electrons from the flavoprotein reduce both cofactors and cause release of the bound phosphate, leading to disorder in the two lysines and two arginines that form the active-site cavity. With one protonated oxygen, sulfite then binds to the distal face of the siroheme through its sulfur while Arg153 flips and orders the loop at the top of the active-site cavity. The unprotonated oxygens form hydrogen bonds with an ordered water molecule at the corner of the cavity. The protein side chains deliver a second proton, a water molecule leaves, and the two-electron reduced sulfur-containing intermediate remains bound to the siroheme, its two remaining oxygens forming hydrogen bonds with the ordered water molecule. Two more electrons come from the flavoprotein through the cofactors and two more protons come from either the protein's side chains or the ordered water molecules while Arg153 flips back to its original orientation. A water molecule leaves from the dioxygen intermediate. The four-electron reduced sulfur-containing species remains bound to the siroheme, its last oxygen forming a hydrogen bond to an ordered water molecule in the active-site cavity. Arg153 remains in its unflipped position. In the penultimate step, the last two electrons and last two protons pass to the substrate, a water molecule leaves, and the six-electron reduced sulfur atom remains bound to the siroheme. Finally, the last proton is delivered and the product (SH^-) leaves. Either a phosphate binds and the enzyme waits for activation by two reducing equivalents, or two electrons pass directly to the metal cofactors, priming the enzyme for substrate binding.

Inhibitors

Carbon monoxide and cyanide both bind to and inhibit the reduced hemoprotein when added before the substrate. When they bind, the EPR and optical spectra change to those characteristic of low-spin heme irons, suggesting that the inhibitors affect the redox and spin states of the cofactors.[6] According to the crystal structures of the complexes, the small molecules bind through their carbon atoms to the Fe_S, nearly perpendicular to the plane of the siroheme nitrogens but slightly tilted towards Arg83, as predicted by the RR spectroscopy (Figure 8).[29,36] The crystals were grown in hepes buffer and the inhibitors were soaked into the Cr(II)EDTA-reduced crystals. During refinement, the metal centers were treated as if they were fully reduced. In the CN^- structure, however, extra density on the distal face of the heme suggests that the anion binds in more than one conformation. The interpretation of the RR studies related the mixture of binding modes to a mixture of redox states in the metals, but the single-crystal EPR spectra do not show a large population of oxidized molecules.[29,36]

CN^- and CO are isoelectronic, but differ in charge and in the extent to which their π-orbitals backbond with the d-orbitals from the Fe_S, as evidenced by subtle differences in their binding to the siroheme that affect the cluster–siroheme–ligand couple. The nitrogen from the cyanide molecule directly hydrogen bonds with Lys215N_ζ and with Arg83N_η, as well as forming water-mediated hydrogen bonds with a propionate group from the siroheme and with Arg153N_ε. In the CO-bound structure, Arg83 is twisted away from the active site and does not interact with CO. Arg153 shifts relative to its position in the cyanide-bound

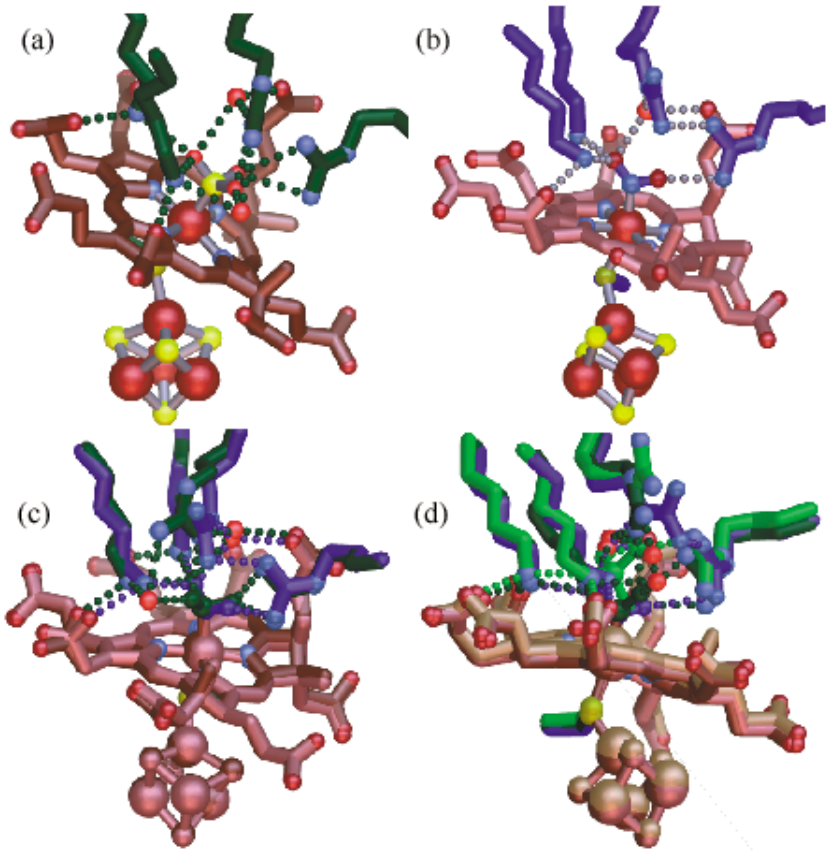

Figure 9 (a) Distal and proximal face of the sulfite-bound active site. Irons are large red spheres, sulfurs are yellow spheres, siroheme is brown, oxygens are red balls, nitrogens are blue balls, sidechains are dark green, waters are red balls, and hydrogen bonds are dark green. (b) Distal and proximal face of the nitrite-bound active site. Irons are large red spheres, sulfurs are yellow spheres, siroheme is pink, oxygens are red balls, nitrogens are blue balls, sidechains are dark blue, and hydrogen bonds are gray balls. (c) Overlay of the sulfite- and nitrite-bound structures (sulfite-bound are dark and nitrite-bound are light). (d) Overlay of the sulfite-, nitrite-, and phosphate-bound structures (sulfite-bound sidechains and anion are dark green and the cofactor are brown; nitrite-bound sidechains and anion are blue and the cofactors are pink; phosphate-bound sidechains and anion are light green and the cofactors are creme). Figures made in AVS.

structure and the water-mediated hydrogen bond between its N_ε and the oxygen from CO is long (about 3.4 Å); the water-mediated hydrogen bond with the propionate group of the siroheme is like that in the cyanide complex. The hydrogen bond with Lys215 is not formed; as a result, the CO is bent by about 3° less than CN^-. Two chemical properties of the carbon monoxide moiety influence its binding mode. First, CO is neutral, hence the hydrogen bonds it forms with the charged side chains are longer and less ordered than when the anionic cyanide molecule is bound. Second, oxygen is more electronegative than nitrogen, therefore CO is a stronger π-acid than CN^- and more electron density will be shared between the Fe_S's d-orbitals and CO's π^*-orbital. The structural consequence of the much more positive iron is a tighter interaction between Fe_S and CO, realized in a shorter C–Fe_S bond in the CO-bound structure than in the CN^--bound structure (1.62 and 1.84 Å, respectively). In both structures, the Fe_S–Cys483 S_γ bond length is 2.23 Å but in the CO structure the whole cluster seems to be shifted towards the siroheme, perhaps another consequence of the more electronegative oxygen atom.

Substrates

Over the course of days, sulfite and nitrite will both exchange with the distally bound phosphate, either in solution or in a crystal, generating a complex that has the same optical spectra as have the complexes formed by first reducing the protein before introducing the substrate.[30] Structures of the sulfite and nitrite bound enzymes were obtained by soaking the fully oxidized crystals with Na_2SO_3 or $NaNO_2$ for two days.

Sulfite binds to Fe_S through its sulfur with a bond length of about 2.2 Å, bringing the oxygen atoms about 1 Å closer to the siroheme than are the phosphate oxygens in the resting state structure (Figure 9(a) and (d)).[36] As a

result of sulfite binding, three loops (residues 127–131, residues 146–152, and residues 184, 185, and 204–109) coalesce around the active site to maintain the network of hydrogen bonds among the positively charged residues, ordered water molecules within the cavity, siroheme propionate groups, and the distally bound ligand. A water molecule not seen in the phosphate-bound structure sits in the far corner of the distal cavity and mediates hydrogen bonds between SO_3's O1 and both a propionate from the siroheme and $N_{\eta 1}$ from Arg153. O1 from the sulfite molecule also forms hydrogen bonds with the N_ζs from Lys215 and Lys217, and with Arg153 N_η. Both of Arg83's N_ηs form direct hydrogen bonds with SO_3's O2, which also forms a water-mediated hydrogen bond with Arg153 N_η through the same ordered water molecule that interacts with O1. The S–O3 distance is about 0.2 Å longer than for the other oxygens, suggesting that it is protonated and the S–O bond is ready to break. The proton could be donated by the ordered water molecule that mediates the hydrogen bond with Arg153 N_η, as it sits about 2.7 Å from the sulfite oxygen in a channel leading to the solvent accessible surface. Lys215 also forms a hydrogen bond with O3.

The most significant structural difference between the sulfite- and phosphate-bound structures is the flipping of Arg153. Unlike the substrate, which binds through its central atom, phosphate binds to the Fe_S through one of its oxygens. Consequently, the phosphate fills the whole space distal to the siroheme and precludes either positioning an ordered water molecule in the far corner of the binding pocket or orienting Arg153's guanidinium group towards the active site. Instead, the guanidinium group points away from the active site, forming a hydrogen bond with Met151 S_δ and presenting its N_ε to interact with the bound anion. Sulfite binding opens space in the active site because the sulfite binds through its central atom and causes the iron to switch from high spin to low spin, reducing the doming of the Fe_S above the siroheme nitrogen plane by about 0.11 Å. Arg153 flips to fill the space, breaking a hydrogen bond with Met151 and allowing the loop in which the methionine is found to order around the active site. As a result of the loop rearrangement, the four main active-site residues (Arg83, Arg153, Lys215, and Lys217) are completely shielded from solvent when substrate is bound.

Like sulfite, nitrite binds to the Fe_S though its central atom, switching the spin state of the iron from high to low and pushing the iron into the plane of the siroheme nitrogens so that the siroheme is only domed by about 0.08 Å (Figure 9(b) and (c)).[36] The O1 forms a direct, long hydrogen bond with Arg83's $N_{\eta 2}$ and O2 forms a direct hydrogen bond with Lys217 as well as a water-mediated hydrogen bond with Arg153's N_ε. Arg153 does not flip in the NO_2^--bound structure, therefore Arg153's terminal N_ηs point away from the active site and play no role in binding the substrate. The two ordered water molecules seen in the sulfite structure (one in the channel from the active site to the solvent accessible surface and the other at the back of the active site) are also present in the NO_2^--bound structure, however there is no ligand oxygen with which the water can hydrogen bond. As a result, it sits further from the active site and closer to the bulk solvent.

Intermediates and other complexes

Native crystals soaked anaerobically with Na_2S generated a structure of a possible reaction intermediate.[36] Extra density suggests that the bound species is not product but some partially oxidized sulfur-containing species, perhaps SO^{2-} or S_2^{2-}, however the exact chemical composition is not defined. If the diatomic molecule is SO^-, then the active site can stabilize an otherwise unstable and transient intermediate that may lie along the reaction pathway, however no such intermediate has been spectroscopically characterized. The only spectroscopically characterized intermediate lies along the pathway of nitrite reduction to ammonia. Structurally, this intermediate was obtained by photoreducing crystals with bound NO_2^-. The resulting structure showed a bent diatomic molecule (the Fe_S–N–O angle was 125°), suggesting that NO^- rather than NO was bound to the heme. The oxygen pointed between the N_ζs from Lys215 and Lys217, forming long hydrogen bonds with each. The Fe_S–S_γ distance in the sulfur adduct is about 0.2 Å longer than in the nitrite-bound complex; however in both complexes the position of the iron within the siroheme is consistent with a low spin iron heme. The structure of another complex was obtained by soaking hydroxylamine into the crystals. The electron density on the distal face of the heme was trigonal planar and not coordinated to the Fe_S. The mother liquor from the crystal was analyzed for nitrogen content and found to contain nitrate and nitrite, thus the density was treated as a molecule of nitrate bound in the distal cavity but not, coordinated to the siroheme. In the structure, nitrate is positioned in the active site like the phosphate molecule, except that the fourth oxygen is absent in nitrate thus the molecule does not coordinate the Fe_S. The position of the iron within the siroheme is consistent with a high-spin configuration. The nitrate is not likely a reaction intermediate and could be a product of hydroxylamine oxidation during the soak.

Redox gating

Although binding to the oxidized enzyme is slow, substrates and inhibitors bind rapidly to the reduced enzyme. The optical properties of the substrate-bound, oxidized enzyme and the substrate-bound, reduced enzyme are identical,[37] and an explanation for the phenomenon was suggested by comparing the structures of the oxidized and reduced enzymes.[36] Phosphate is bound to the

oxidized but not to the reduced siroheme, so the different binding kinetics can be attributed to a redox-gated steric block in the oxidized enzyme's active site and not to a different mode of substrate binding.

CONCLUSIONS

The structure of SiRHP realizes several themes that add to our understanding of heme-containing metalloproteins by linking spectroscopic activity with the structural changes in the active site of the enzyme. The relationship between each half of the aSiRHP, the individual subunits of dSiRs, and NiRs suggests that a structural motif called the SNiRR is an evolutionary unit that is well suited for selective binding and efficient catalysis of small anionic molecules. The flexible residues that crown the active site and the phosphate that is bound to the active site of the resting enzyme suggest two types of conformational change that are associated with catalysis. First, the reduction of cofactors triggers the phosphate release needed for substrate binding. Second, on sulfite binding, the active site tightens to maintain a regular pattern of hydrogen bonds with the bound ligand. The flexible active site and the conformational change in the loop triggered by substrate binding suggests that the rapid and efficient catalysis is related to ligand binding and the order it imbues on the active site. The dramatic *trans* effect of ligands binding to the distal face of the siroheme on the structure and spin state of the Fe_S indicate that the electronic couple between the [4Fe–4S] cluster extends through the substrate, and the energetic relationship of bonding and antibonding orbitals in the cluster relates to those in the substrate. For example, density functional calculations suggest that one-electron reduced [4Fe–4S] clusters house the extra electron in a π-antibonding orbital.[38] Backbonding with between the Fe_S and the distally bound ligand would pull electron density out of the cluster's antibonding orbitals, through the couple siroheme, and into the antibonding orbitals of the substrate, weakening the substrate's bonds and preparing them for cleavage.[35]

NOTE ADDED IN PROOF

Recent biochemical studies performed on a 1:1 complex of truncated flavoprotein to hemoprotein show that this simplified version of SiR is functional. These studies have brought into question the actual stoichiometry of the holoenzyme complex, with a citation to M Zeghouf, M Fontecave and J Coves, *J Biol Chem*, 48, 37651–6 (2000).

ACKNOWLEDGMENTS

We kindly thank M. DiDonato, C.D. Putnam, and B.R. Crane for their helpful comments on the manuscript. Funding was provided by a National Science Foundation fellowship to MES and the National Institute of Health, grant GM37684.

REFERENCES

1 LM Siegel, MJ Murphy and H Kamin, *J Biol Chem*, **248**, 251–64 (1973).

2 HD Peck and T Lissolo, in JA Cole (ed.), *Symposium of the Society for General Microbiology – The Nitrogen and Sulfur Cycles*, Cambridge University Press, Cambridge, pp 99–132 (1988).

3 BR Crane and ED Getzoff, *Curr Opin Struct Biol*, **6**, 744–56 (1996).

4 R Hell, *Planta*, **202**, 138–48 (1997).

5 LM Siegel, *Biochemistry of the sulfur cycle*, Metabolic Pathways, Academic Press, New York (1975).

6 LM Siegel, DC Rueger, MJ Barber, RJ Krueger, NR Orme-Johnson and WH Orme-Johnson, *J Biol Chem*, **257**, 6343–50 (1982).

7 BR Crane, LM Siegel and ED Getzoff, *Science*, **270**, 59–67 (1995).

8 J Ostrowski, MJ Barber, DC Rueger, BE Miller, LM Siegel and NM Kredich, *J Biol Chem*, **264**, 15796–808 (1989).

9 J Ostrowski, JY Wu, DC Rueger, BE Miller, LM Siegel and NM Kredich, *J Biol Chem*, **264**, 15726–37 (1989).

10 T Haverkamp and JD Schwenn, *Microbiology*, **145**, 115–25 (1999).

11 C Bork, JD Schwenn and R Hell, *Gene*, **212**, 147–53 (1998).

12 G Gisselmann, P Klausmeier and JD Schwenn, *Biochim Biophys Acta*, **1144**, 102–6 (1993).

13 T Kaneko, S Sato, H Kotani, A Tanaka, E Asamizo, Y Nakamura, N Miyajima, M Hirosawa, M Sugiura, S Sasamoto, T Kimura, T Hosouchi, A Matsuno, A Muraki, N Nakazaki, K Naruo, S Okumura, S Shimpo, C Takeuchi, T Wada, A Watanabe, M Yamada, M Yasuda and S Tabata, *DNA Res*, **3**, 109–36 (1996).

14 J Tan, LR Helms, RP Swenson and JA Cowan, *Biochemistry*, **30**, 9900–7 (1991).

15 JY Wu, LM Siegel and NM Kredich, *J Bacteriol*, **173**, 325–33 (1991).

16 MJ Warren, CA Roessner, PJ Santander and AI Scott, *Biochem J*, **265**, 725–9 (1990).

17 M Eschenbrenner, J Coves and M Fontecave, *FEBS Lett*, **374**, 82–4 (1995).

18 DE McRee, DC Richardson, JS Richardson and LM Siegel, *J Biol Chem*, **261**, 10277–81 (1986).

19 SC Woodcock, E Raux, F Levillayer, C Thermes, A Rambach and MJ Warren, *Biochem J*, **330**, 121–9 (1998).

20 M van de Bogart and H Beinert, *Anal Biochem*, **20**, 325 (1967).

21 MJ Murphy, LM Siegel, H Kamin and D Rosenthal, *J Biol Chem*, **248**, 2801–14 (1973).

22 RJ Krueger and LM Siegel, *Biochemistry*, **21**, 2892–904 (1982).

23 JA Christner, E Munck, PA Janick and LM Siegel, *J Biol Chem*, **256**, 2098–101 (1981).

24 S Han, JF Madden, RG Thompson, SH Strauss, LM Siegel and TG Spiro, *Biochemistry*, **28**, 5461–71 (1989).

25 JF Madden, SH Han, LM Siegel and TG Spiro, *Biochemistry*, **28**, 5471–7 (1989).

26 PA Janick and LM Siegel, *Biochemistry*, **21**, 3538–47 (1982).

27 JA Christner, E Munck, PA Janick and LM Siegel, *J Biol Chem*, **258**, 11147–56 (1983).

28 JA Christner, PA Janick, LM Siegel and E Munck, *J Biol Chem*, **258**, 11157–64 (1983).

29 SH Han, JF Madden, LM Siegel and TG Spiro, *Biochemistry*, **28**, 5477–85 (1989).

30 PA Janick, DC Rueger, RJ Krueger, MJ Barber and LM Siegel, *Biochemistry*, **22**, 396–408 (1983).

31 LJ Young and LM Siegel, *Biochemistry*, **27**, 5984–90 (1988).

32 AM Stolzenberg, SH Strauss and RH Holm, *J Am Chem Soc*, **103**, 4763–78 (1981).

33 BR Crane, H Bellamy and ED Getzoff, *Acta Cryst D*, **52**, 8–22 (1997).

34 BR Crane, H Bellamy and ED Getzoff, *Acta Cryst D*, **52**, 23–40 (1997).

35 BR Crane, LM Siegel and ED Getzoff, *Biochemistry*, **36**, 12120–37 (1997).

36 BR Crane, LM Siegel and ED Getzoff, *Biochemistry*, **36**, 12101–19 (1997).

37 PA Janick, DC Rueger, RJ Krueger, MJ Barber and LM Siegel, *Biochemistry*, **22**, 396–405 (1983).

38 L Noodleman and DA Case, *Adv Inorg Chem*, **38**, 423–69 (1992).

39 LJ Young and LM Siegel, *Biochemistry*, **27**, 4991–9 (1988).

40 C Upson, T Faulhabe, D Kamins, D Laidlaw, D Schlegel, J Vroom, R Gurwitz and A Vandam, *IEEE Comp G*, **9**, 30–42 (1989).

41 R Sayle and EJ Milner-White, *TIBS*, **20**, 333–79 (1995).